

NOTICE

**CERTAIN DATA
CONTAINED IN THIS
DOCUMENT MAY BE
DIFFICULT TO READ
IN MICROFICHE
PRODUCTS.**

The Effects of Laser Beam Non-uniformities on X-ray Conversion Efficiency

Steven Langer and Kent Estabrook

UCRL-JC--105307

Lawrence Livermore National Laboratory¹

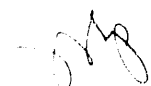
DE91 004879

Introduction

High gain Inertial Confinement Fusion (ICF) targets require a highly uniform drive. In the case of direct drive, the inherent non-uniformities in a high-power glass laser beam are large enough to prevent high compression of targets. In recent years two methods for smoothing the laser drive, Induced Spatial Incoherence (ISI) and Smoothing by Spectral Dispersion (SSD), have been proposed. Both methods break the original laser beam up into many beamlets that then interfere at the target to produce an illumination pattern with large instantaneous intensity variations over a wide range of spatial scales. This interference pattern dances around at the coherence time of the laser and averages out to produce a smooth beam on longer time scales. Transport processes help to smooth out the short spatial wavelength variations in the intensity, which would otherwise cause problems.

Indirect drive schemes shine the laser on a high-Z material, usually gold, which converts the laser energy into x-rays. The x-rays are then used to drive the target. Non-uniformities in the laser beam can imprint themselves on the emitted x-rays and potentially cause problems, although the spatial transport of the x-rays to the target tends to smooth out these

¹Work performed under the auspices of the U.S. Department of Energy by the Lawrence Livermore National Laboratory under Contract W-7450-ENG-48.

MASTER 
DISTRIBUTION OF THIS DOCUMENT IS UNLIMITED

non-uniformities. As a result, ISI and SSD schemes are also being considered for indirect drive laser systems.

We address this problem by modeling the effects on the x-ray conversion efficiency of shining a laser beam with a sinusoidal intensity modulation on a gold slab. Our principal results are that electron heat transport is quite efficient in smoothing out non-uniformities in the laser deposition before they reach the ablation surface if the spatial scale of the laser modulation is less than roughly 500 μm . We also show that the gold plasma is below the Raman and Brillouin thresholds throughout the pulse.

Method of Solution

The LASNEX computer code is used to simulate the effect of a sinusoidal laser intensity modulation across the face of a gold on the x-ray conversion efficiency (CE). The mean laser intensity is $5 \times 10^{14} \text{ W/cm}^2$ of 3 ω (blue) light. The laser pulse is a 1 ns flattop. For the first 500 ps the laser intensity is nominally uniform across the slab. After that point the total laser power is held constant, but a sinusoidal spatial modulation is applied. The spatial wavelength of this modulation is called λ_{\perp} . A new set of laser ray directions is chosen randomly within a cone of $\pm 5.7^{\circ}$ around the slab normal on each cycle. The laser package in LASNEX tracks laser rays through the mesh and deposits energy along the track. The goal of choosing new ray directions on each cycle is to randomize the effects of discrete rays depositing in discrete zones and thus producing non-uniform heating even for a nominally uniform beam. A similar scheme could be used to mimic the effects of ISI or SSD if the ray directions were re-chosen once every laser coherence time.

The problem we solve has, conceptually, a laser intensity that varies

sinusoidally in one direction across an infinite slab and has no variation in the other direction. By symmetry, the models only need to cover half a wavelength of the laser modulation (from a maximum intensity to a minimum). Our models used 10 zones in the transverse direction and 123 zones in the direction into the slab. The laser deposition region was well resolved, but better resolution at the steepest part of the ablation front is desirable. Figure 1 is a sketch of the geometry and indicates how the laser intensity varies across the slab.

Results

Figure 2 shows contours of the laser deposition 200 ps after the laser intensity modulation has been turned on. The intensity varies from 2 to 8×10^{14} W/cm², for an intensity ratio of 4:1 with $\lambda_{\perp} = 50$ μ m. The laser power remained the same as earlier in the run. The laser deposition follows the intensity modulation. At this time, the peak laser deposition is roughly 60 μ m outside of the ablation front, so it is possible to smooth out the heat flux on the scale of λ_{\perp} .

Figure 3 shows temperature contours at the same time. The contours are nearly parallel to the original slab surface, indicating that strong smoothing has occurred. Figure 4 shows the same contours when λ_{\perp} is 1000 μ m. In this case there is very little smoothing (the different parts of the slab act like independent 1D problems with different laser intensities).

Brueckner and Jorna (1974) made a rough estimate showing that electron heat conduction should be able to smooth out variations on a distance scale δx in a time δt when the two are related by:

$$\delta x = 183 \frac{\lambda}{1/3 \mu\text{m}} \left(\frac{\delta t}{1 \text{ ns}} \frac{n_c}{n_e} \right)^{1/2} \left(\frac{T_e}{1 \text{ keV}} \right)^{5/4} \mu\text{m}$$

where λ is the wavelength of the laser. For the case we are considering, the variations need to be smoothed out on the time scale that new plasma flows from the ablation front to the laser deposition region. Basing the estimate on the 3 keV temperature, $2.5 \times 10^{21} \text{ cm}^{-3}$ electron density and z_{bar} of 55 at the peak deposition point, the sound speed is roughly $370 \mu\text{m/ns}$. This means it will take roughly 0.16 ns to flow the $60 \mu\text{m}$ from the ablation front to the peak deposition point. The formula suggests that variations should be smoothed out on distance scales shorter than roughly $550 \mu\text{m}$. We observe strong smoothing for $\lambda_{\perp} = 50 \mu\text{m}$ and very little smoothing for $\lambda_{\perp} = 1000 \mu\text{m}$ in the LASNEX simulations, in reasonable agreement with the simple theory.

Figure 5 shows the amplitude of the bend in the ablation front as a function of time for several runs. In this case we define the ablation front as that point where the electron temperature is 400 eV (other definitions produce similar results). The two runs with $\lambda_{\perp} = 50 \mu\text{m}$ never develop an amplitude larger than roughly $1 \mu\text{m}$. The run with a 4:1 laser variation has an amplitude roughly 50% greater than the run with a 2:1 laser variation. The run with $\lambda_{\perp} = 1000 \mu\text{m}$ develops a separation in excess of $20 \mu\text{m}$ by the end of the laser pulse at 1.1 ns. The $\lambda_{\perp} = 1000 \mu\text{m}$ run has a separation nearly identical to the separation between two 1D runs with the minimum and maximum laser intensities of the 2D run. This shows that for $\lambda_{\perp} = 1000 \mu\text{m}$, electron heat conduction has little smoothing effect inside the critical density. Contours of the electron temperature show that even well outside

of the critical surface the temperature is not uniform.

The bending of the ablation front will increase linearly with time if the difference in the velocity of the ablation front is constant. The bending actually increases more slowly as time goes on, which is reasonable given that the separation between the ablation front and the deposition region increases with time and makes it easier to smooth out the variation in laser deposition.

Figure 6 shows the fractional difference in x-ray intensity between the two sides of the disk as a function of time in two spectral bands. The intensity is in the direction of the slab normal and is calculated using a post-processor. Curves are shown for both $\lambda_{\perp}=50 \mu\text{m}$ and $1000 \mu\text{m}$ with an intensity ratio of 4:1. The modulation is a few percent for the $\lambda_{\perp}=50 \mu\text{m}$ run and does not change significantly during the laser pulse. There is a good chance that most of this variation can be traced to the discreteness of the zoning. The variation is quite pronounced for the $\lambda_{\perp}=1000 \mu\text{m}$ run, with the amplitude decreasing steadily in the 800 eV band and having a maximum in the 2.7 keV band roughly 200 ps after the laser modulation is turned on. The delayed peak at 2.7 keV is probably due to the time required to build up plasma at the higher temperatures made possible by the new peak intensity. The decreasing amplitude of the spatial variation in the x-rays is in agreement with the decreasing difference in the ablation front velocity. The ratio in amplitude between the two runs is hard to define, given that lack of any clear trend for the $\lambda_{\perp}=50 \mu\text{m}$ run. The total conversion efficiency is essentially identical for both runs (48.4% to 48.8% at 950 ps), and is the same as is found in a uniform intensity run.

Plasma Instabilities

We have used the P³ post-processor code to check whether the ablated gold plasma is above threshold for any of the common plasma instabilities. For all of the models we have run, the amount of Raman and Brillouin radiation is zero. Some $2\omega_p$ instability is present, but at very low levels. These results are not surprising because gold is highly collisional and the peak intensity, even for the 4:1 models, is only 8×10^{14} W/cm². Longer pulse lengths, such as those suggested for reactor scale targets, will be more prone to plasma instabilities.

Conclusions

We have shown that electron heat conduction greatly smooths non-uniform laser deposition for spatial scales smaller than roughly 500 μm for this intensity. The smoothing is less pronounced in the x-ray emission than in the bending of the ablation front. None of our models, all of which had peak intensities less than 8×10^{14} W/cm², showed significant plasma instabilities. In future work, we intend to consider more transverse wavelengths and the effects of several simultaneous wavelengths such as would be present in ISI or SSD schemes. We will also consider higher intensities, other slab materials, and longer pulse lengths if there is sufficient interest.

References

Keith A. Brueckner and Siebe Jorna, 1974, Rev. Mod. Phys. **46**, 325.

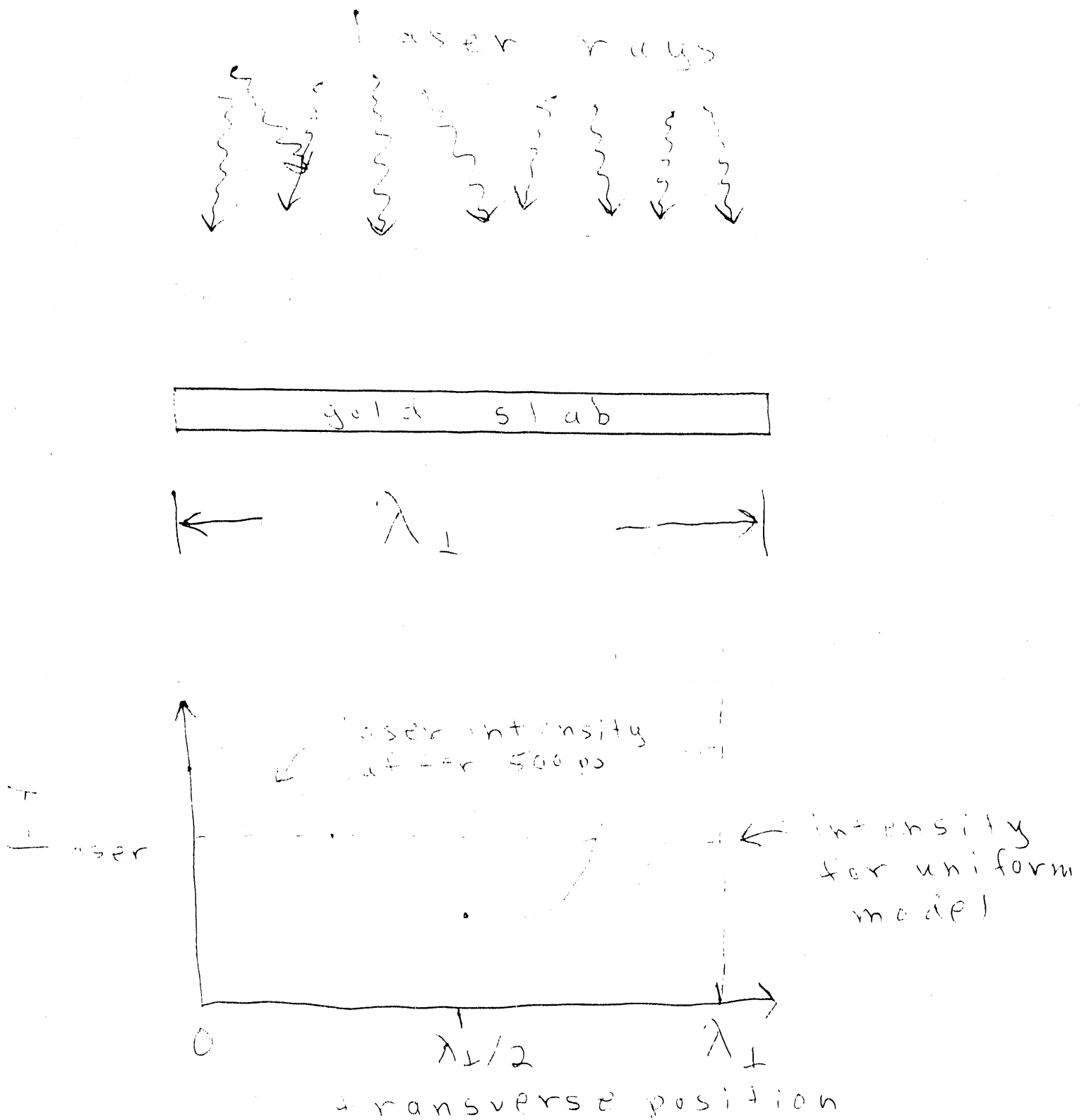


Figure 1. This figure shows the geometry used for our models. The models cover half a wavelength of the laser intensity modulation. The lower figure shows the intensity variation across the face of

time=.7007420008263 ns. job isi07

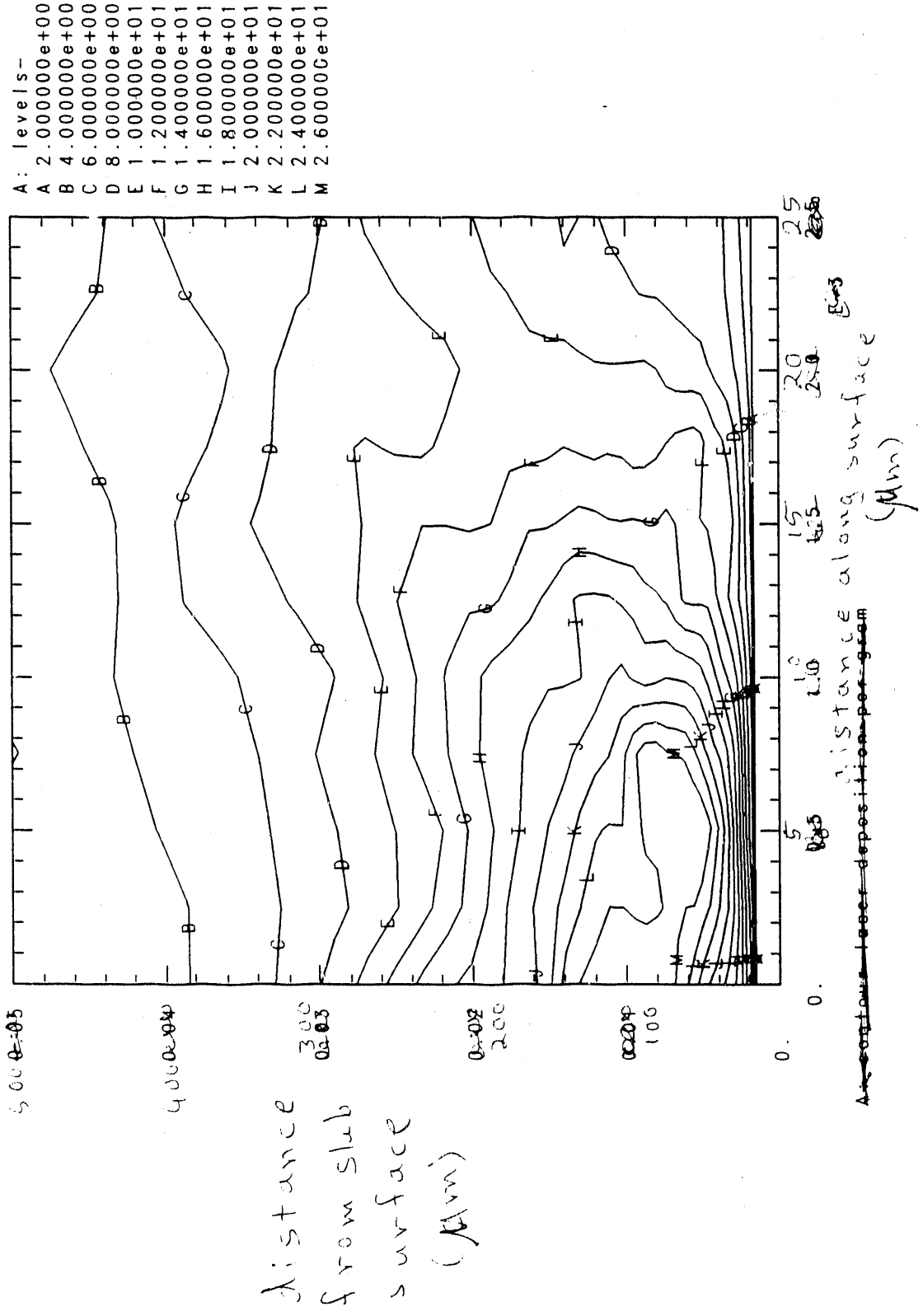
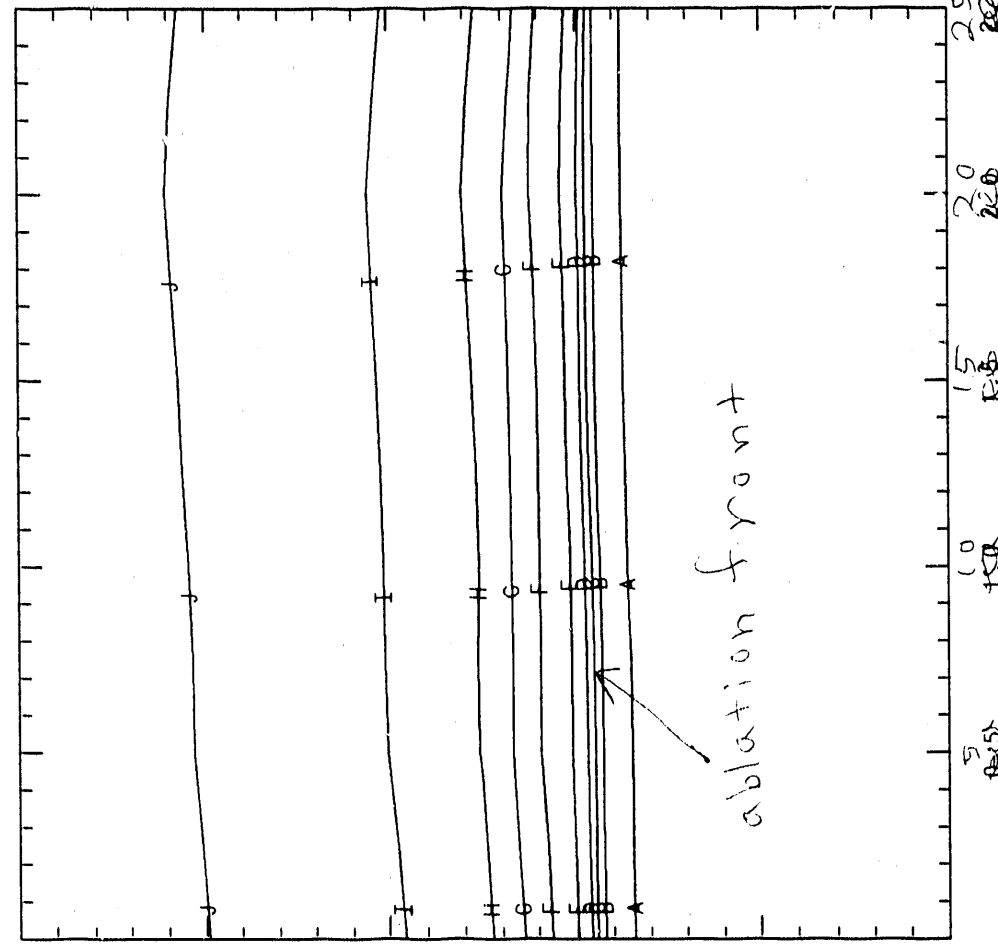


Figure 2. Contours of ~~contour~~ the rate of deposition of laser energy per gram of material are shown for a $\lambda = 50 \mu\text{m}$ slab with a 4:1 intensity ratio. This is a snapshot taken 200 ps after the 4:1 intensity variation was turned on

time=.7007420008263 ns, job isi07

A: levels-
 A 2.000000e-01
 B 3.000000e-01
 C 4.000000e-01
 D 5.000000e-01
 E 7.000000e-01
 F 1.000000e+00
 G 1.200000e+00
 H 1.400000e+00
 I 1.700000e+00
 J 2.000000e+00



30 300

25 250

20 200

Distance from slab surface (μm)

15 150

10 100

ablation front

5 50

0.

5 10 15 20 25

A: contour temperature distance along slab (μm)
 Figure 3. Contours of the electron temperature at the same time as Fig. 2. The temperature and other plasma properties show little effect of the large difference in deposition seen in fig. 2.

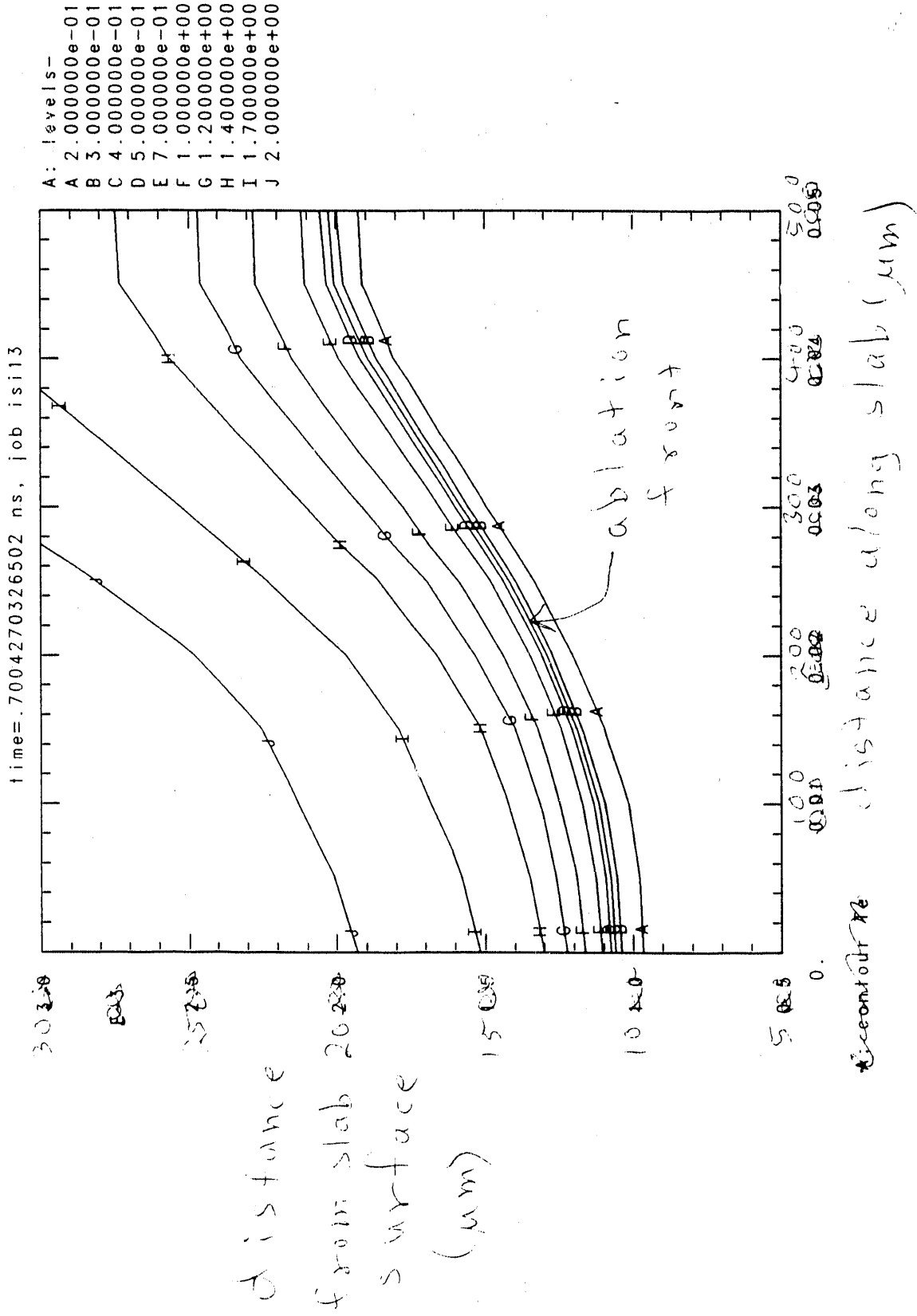


Figure 4. Same as fig. 3 except $\eta_1 = 1000 \mu\text{m}$. The ablation front and all other contours were strongly bent.

ablation front bending (μm)

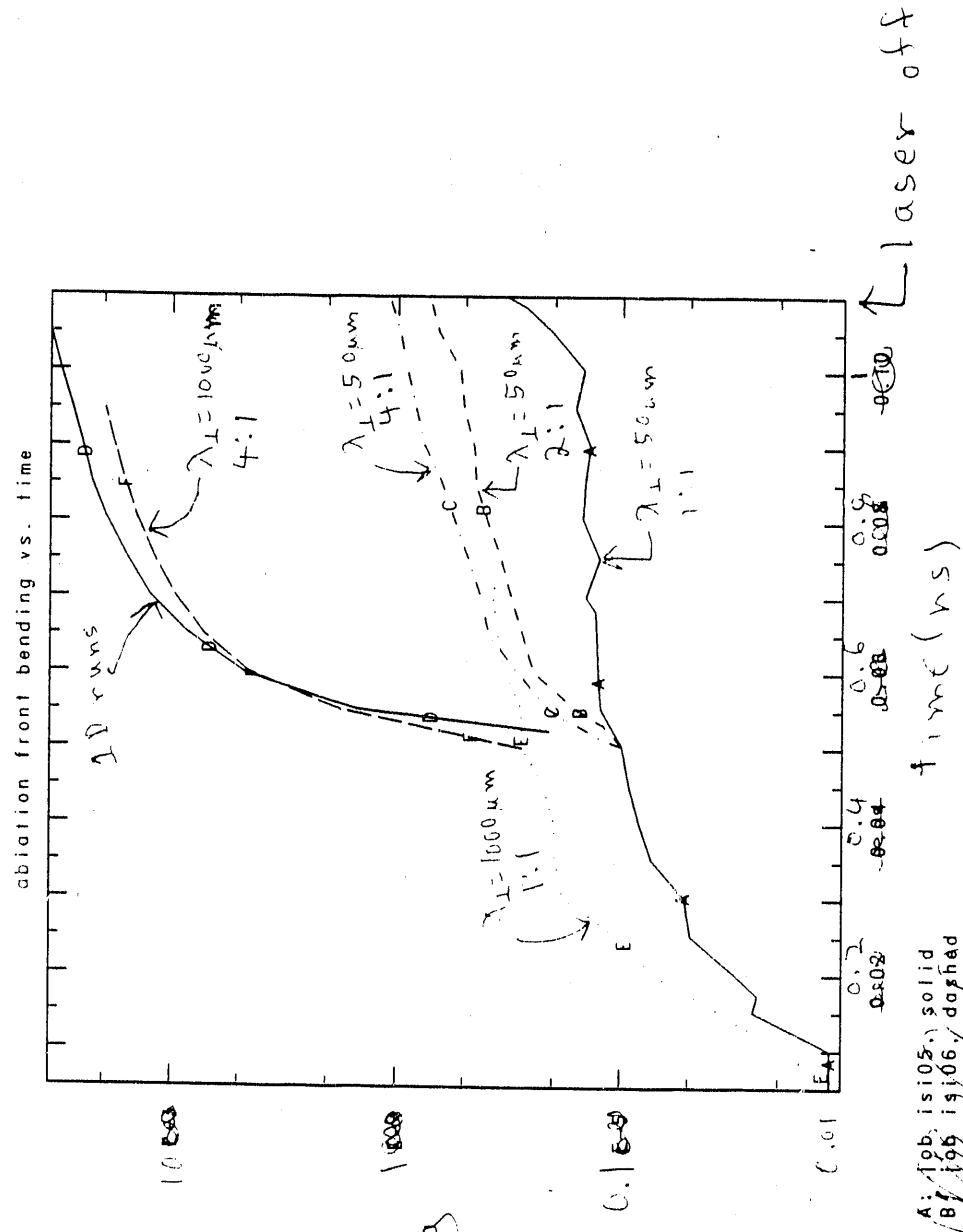
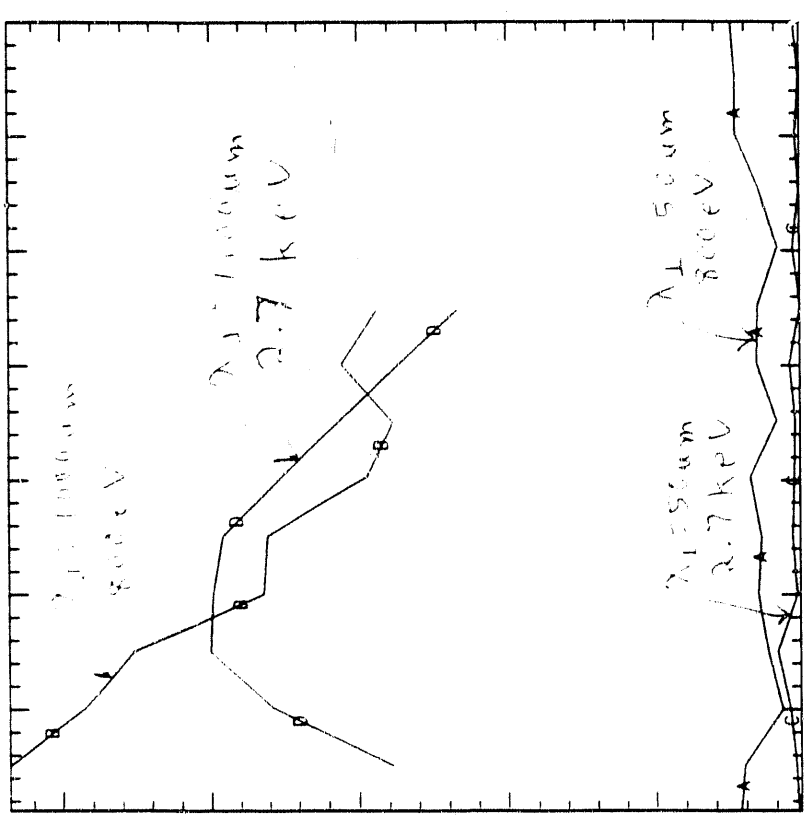


Figure 5. The ablation front bending

is shown as a function of time for several models labeled by λ_I and the laser intensity ratio. The sharp turn on at the laser variation is apparent. The bending for $\lambda_I = 1000 \mu\text{m}$ is only slightly smaller than ~~the~~ the difference in ablation front position for two 1D models run with the minimum and maximum laser intensity used in the 2D model. This shows that there is little smoothing in the $\lambda_I = 1000 \mu\text{m}$ case

Handwritten title: $\lambda_{I=50\mu m}$ vs $\lambda_{I=800eV}$



Fractional variation in X-ray intensity $\left(\frac{\text{max} - \text{min}}{\text{avg}} \right)$

0.6 0.8 1.0 1.2
 time (ms)
 A: .8024604053352 to .8914150667278 ev, solid, job isi07
 B: .8024604053352 to .8914150667278 ev, dashed, job isi13
 C: 2.588736589364 to 2.919244136618 ev, solid, job isi07
 D: 2.588736589364 to 2.919244136618 ev, dashed, job isi13

Figure 6. The curves show the fractional variation in X-ray brightness between the two sides of the slab. The $\lambda_{I=50\mu m}$ model shows easily measurable variations. Part of the large early variation at $\lambda_{I=50\mu m}$ and 800eV is due to emission before the temperature and density profile has a chance to settle down to the new laser intensity. The lag at 2.7 keV is a measure of how long it takes to build up the hot, lower density plasma that emits the M-band radiation. The $\lambda_{I=50\mu m}$ model is nearly uniform.

END

DATE FILMED

12 / 31 / 90

